CMS Physics Analysis Summary

Contact: cms-pag-conveners-exotica@cern.ch 2020/07/23

Search for Strongly Interacting Massive Particles with Trackless Jets

The CMS Collaboration

Abstract

A search for dark matter in the form of strongly interacting massive particles, manifesting themselves as a pair of jets without tracks in the CMS detector at the LHC, is presented. The charged energy fraction of jets is used as a key discriminator to efficiently suppress the large multijet background, and the remaining background is estimated directly from data. The search is performed using proton-proton collision data corresponding to an integrated luminosity of 16.1 fb^{-1}, collected by the CMS detector in 2016. No significant excess of events is observed above the expected background. Strongly interacting massive particles with masses up to 900 GeV are excluded at 95% confidence level for the model under consideration. The presented analysis thus evaluates the sensitivity to an unconventional phase space for new physics for the first time at colliders. In addition to the interpretation in the context of the SIMP model, model-independent limits that can be used for reinterpretation of the results are provided.

1 Introduction

The searches at the CERN LHC for physics beyond the standard model are broad and diverse. In particular, an extensive program has been developed to search for dark matter, the precise nature of which is one of the main open questions in particle physics. These searches for dark matter typically focus on a weakly interacting massive particle (WIMP) with a mass around the electroweak scale. Such a particle can naturally account for the measured dark matter abundance in the universe, assuming thermal dark matter production in the ΛCDM standard cosmological model [1, 2]. If produced at the LHC, such a WIMP would, like a neutrino, be undetectable in the experiments, and would give rise to signatures with missing transverse momentum (p_{T}).

Due to the lack of any compelling evidence for the existence of WIMP dark matter—despite many searches probing the plausible WIMP parameter space—many theoretical developments now venture beyond the minimal WIMP model or alter its basic assumptions. In this analysis, we consider the possibility that dark matter is produced at the LHC, and that its interaction cross section with normal matter is so high that the particles are no longer WIMPs, but become SIMPs or strongly interacting massive particles. Such particles could be copiously produced at the LHC, and leave observable signals in the CMS detector. With an interaction cross section as large as the hadronic one, these SIMPs manifest themselves as jets in the calorimeter, but with no tracks in the tracking detector from charged hadrons, in sharp contrast to typical quantum chromodynamics (QCD) jets. While at first sight it may not seem plausible that such a particle would not have been detected before, it is actually possible to construct a simplified model of SIMPs, interacting through a new scalar or vector low-mass mediator, that evades the many relevant existing bounds [3]. One of the requirements is a purely repulsive SIMP-nucleon interaction with opposite-sign couplings to avoid the formation of bound states between SIMPs and nucleons. Constraints stemming from the need to keep the impact of the new interaction on the nuclear potential small limit the coupling strength between the SIMP and nucleons. Furthermore, a scenario with fermionic, asymmetric dark matter must be considered to avoid excessive Earth heating and neutron-star collapse.

The assumed SIMP production process is illustrated in Figure 1. Due to the hadronic nature of the interaction, it is difficult to make precise estimates of the expected trackless jets signature, as also argued in [3]. Rather, the simplified model under consideration is constructed so that it can viably yield this experimental signature for a specific choice of the couplings, tuned such that the SIMP may be detected as an hadronic shower that starts and is contained within the hadronic calorimeter. Stronger couplings would give rise to showers starting earlier, in the tracker or electromagnetic calorimeter, and weaker couplings can lead to late extended showers leaking into the muon system. The considered simplified model serves thus a benchmark model to explore the constrained phase space of pair production of SIMP-induced jets in the CMS hadronic calorimeter. The resulting jets are expected to be neutral, since no hadronisation of the SIMP takes place, apart from the suppressed higher-order process of quarks emanating from a mediator radiated off one of the SIMP particles.

In the analysis presented here, we search for SIMPs yielding trackless jets using a data set of proton-proton collisions at $\sqrt{s} = 13\,\mathrm{TeV}$, corresponding to an integrated luminosity of $16.1\,\mathrm{fb}^{-1}$, collected by the CMS experiment at the LHC in the second half of 2016. In particular, we search for the pair production of SIMPs, using the charged energy fraction (ChF) of the resulting jets as a strongly discriminating observable to suppress the very large QCD multijet background. Since this background is not accurately modeled in simulation, we estimate it from data.

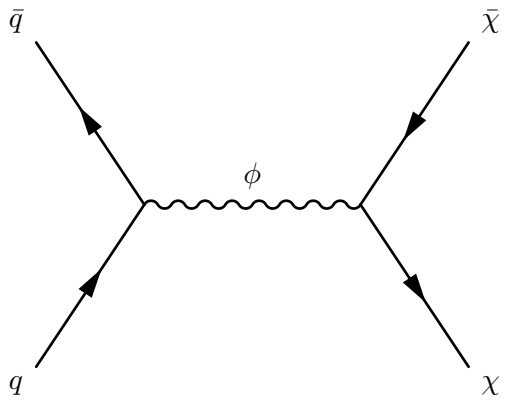

Figure 1: Feynman diagram showing the production of a SIMP pair, through a new low mass mediator.

The ATLAS Collaboration has performed a search for trackless jets before [4]. However, differences in the choice of signal model (decays in the hadronic calorimeter of long-lived neutral particles) and trigger strategy (dedicated so-called *CalRatio* trigger) make a direct comparison difficult. The use of a dedicated trigger on the one hand makes it possible to significantly lower the jet momentum requirements and thus boost the sensitivity. On the other hand, jet showers starting in the electromagnetic calorimeter are penalized, and reduced sensitivity can be expected for SIMP-nucleon interaction cross sections of the level of hadronic cross sections or stronger. Also non-collider experiments have probed similar or nearby phase space, in particular several direct-detection dark matter detectors that were briefly operated at the Earth's surface [5–7]. A direct comparison of these results with collider results may however depend on model assumptions [8, 9].

The analysis here thus evaluates the sensitivity to an unconventional phase space for new physics for the first time at colliders. Apart from the interpretation in the context of the SIMP model, we also provide model-independent limits that can be used for reinterpretation of the results.

2 The CMS detector

The central feature of the CMS apparatus is a superconducting solenoid of 6 m internal diameter, providing a magnetic field of 3.8 T. Within the solenoid volume are a silicon pixel and strip tracker, a lead tungstate crystal electromagnetic calorimeter, and a brass and scintillator hadron calorimeter, each composed of a barrel and two endcap sections. Forward calorimeters extend the pseudorapidity coverage provided by the barrel and endcap detectors. Muons are detected in gas-ionization chambers embedded in the steel flux-return yoke outside the solenoid.

A more detailed description of the CMS detector, together with a definition of the coordinate system used and the relevant kinematic variables, can be found in Ref. [10].

3 Physics object reconstruction

In this analysis, we search for jet-like objects with a very small ChF. To reconstruct and identify these objects, we take as input the charged hadrons, neutral hadrons, photons, electrons, and muons, all of which are coherently reconstructed by the particle-flow event algorithm [11].

Next, we cluster these particles in jets using the anti-k_T algorithm [12, 13] with distance parameter $R = 0.4$, which by construction provides an unambiguous association of tracks to jets. The response of these jets is subsequently corrected for energy contributions from overlapping proton-proton collisions (pileup) and for η- and p_T-dependent response biases [14].

The reconstructed vertex with the largest value of summed physics-object p_T^2 is taken to be the primary pp interaction vertex. The physics objects are the jets, clustered using the jet finding algorithm [12, 13] with the tracks assigned to the vertex as inputs, and the associated missing transverse momentum, taken as the negative vector sum of the p_T of those jets. The tracks are associated with the vertex following the application of a deterministic annealing filter, which assigns weights to sufficiently high-quality tracks that enter the vertex fit [15]. More details are given in Section 9.4.1 of Ref. [16].

While jets with tens of high-momentum tracks can usually be associated with a primary vertex, this is not the case for neutral jets. The underlying event and initial state QCD radiation may provide some tracks, but it is likely that the wrong vertex is selected in signal-like events. In such cases, the event-by-event removal of charged particles not associated with the chosen primary vertex as a means to suppress tracks from pileup vertices also removes the tracks from the SIMP production vertex.

An incorrect choice of vertex is not a problem in the case of signal events, which exhibit a low charged content already. However, a wrongly chosen vertex in a QCD multijet background event causes the pileup suppression procedure to purge the tracks from the true vertex, resulting in the spurious appearance of neutral jets. This makes such an event appear signal-like. For the tightest ChF requirements considered in this analysis, this reconstruction induced background becomes dominant with respect to the background of prompt photons and very rare jet fragmentation into mostly neutral hadrons and photons.

Simulation studies have shown that when the first vertex is wrongly chosen, the second of the ordered list of reconstructed vertices is the true vertex from the hard collision in more than 50% of the cases, often because a single poor-quality track from a pileup collision is erroneously reconstructed with high momentum. Therefore, to mitigate this reconstruction induced background, we use an alternate event reconstruction, assuming the second vertex to be the collision vertex. In case the second vertex is the correct one, the QCD jets acquire larger ChF compared to the default reconstruction. In the event selection discussed later, we can then suppress the background resulting from this effect by enforcing the low jet ChF requirements on both event reconstructions.

Since photons are reconstructed as neutral jets, we need to efficiently identify and reject photons. In this analysis, we identify photons using loose identification requirements [17]. To further increase our photon identification efficiency, we also consider photons failing these requirements but having a reconstructed conversion whose transverse momentum is greater than 30% of that of the photon. Finally, we also require the neutral electromagnetic fraction of jets to be below 0.9 to eliminate genuine photons, which additionally removes spurious jets formed around anomalous ECAL deposits.

4 Simulation

The interaction Lagrangian for a SIMP fermion χ and a vector mediator ϕ

$$\mathcal{L}_{int} = -g_\chi \phi\, \bar{\chi}\chi - g_q \phi\, \bar{q}q, \tag{1}$$

with couplings $g_\chi = -1$ and $g_q = 1$, and mass $m_\phi = 0.14\,\text{GeV}$, is implemented in FEYNRULES 2.0 [18] and interfaced with MADGRAPH5_aMC@NLO [19] to generate SIMP pair events at leading order.

The SIMP signal is simulated for a range of masses. The lowest considered mass is 1 GeV with a production cross section of $\sigma_{\bar{\chi}\chi} = 15.24\,\text{pb}$, obtained for $|\eta(\chi)| < 2.5$ and $p_\text{T}(\chi) > 200\,\text{GeV}$. Using PYTHIA v8.2 [20] and tune CUETP8M1 [21], we then add an underlying event arising from the fragments of the protons that did not participate in the hard collision, and the generated partons are hadronized. The interaction of the resulting particles with the CMS detector is simulated using GEANT4 [22], and pileup collisions are overlayed on the main collision.

The interaction of SIMPs with matter is not implemented in GEANT4. An implementation of the SIMP interaction Lagrangian as a physics model into GEANT could address this, but is highly non-trivial because of possible hadronic physics effects that are not evaluated in the proposal of the simplified model. Incorporating such effects would go beyond the philosophy of providing a simple benchmark for the considered experimental final state.

Therefore, we approximated the SIMPs by neutrons, since the shower induced by the SIMP interaction can be reasonably modeled by the interaction of a high-momentum neutral hadron. This is only approximately so, since the neutron is a composite particle that breaks up in the interaction and ceases to exist, while a SIMP will continue with reduced momentum and induce further interactions.

The assumption of a neutron interaction is only valid for a certain range of couplings. As described in Ref. [3], decreasing the SIMP-nucleon interaction cross section $\sigma_{\chi,N} \sim g_q^2 g_\chi^2$ by a factor 10 reduces the signal acceptance by a factor 6. An increase in cross section, on the other hand, is constrained from above by measurements of the cosmic microwave background. The assumption of a hadron-like interaction cross section with the detector material thus is an apt choice to demonstrate the experimental signature targeted with the simplified model above.

High-mass SIMPs with large incident momenta will transfer little momentum in their collisions with the low-mass nucleons at rest in the detector material, and will thus induce smaller shower energy depositions than if they had a small mass. To capture the kinematics of such collisions in the case of a SIMP with a mass significantly larger than the neutron mass, we added to the simulation a new SIMP particle as a clone of the standard neutron, but with an adjustable mass. With this setup, SIMP signal samples can be coherently simulated and reconstructed, and narrow jets with a large neutral hadron energy fraction are obtained. This SIMP simulation was verified to match the simulation with neutrons for SIMPs with the mass of a neutron, while at high SIMP mass we observe indeed a suppression of the reconstructed energies due to reduced shower depositions. As an example, a SIMP with 1000 GeV mass and $p_\text{T} > 200\,\text{GeV}$ leads on average to a jet momentum about half as large as a nearly massless SIMP.

The main QCD multijet background is also simulated using MADGRAPH5_aMC@NLO with the same PYTHIA tune CUETP8M1 for the underlying event.

5 Event selection

This analysis used only a portion of the data collected during 2016 because, for the early part of that running period, saturation-induced dead time was present in the readout of the silicon strip tracker. This caused hard-to-model instantaneous luminosity-dependent inefficiencies for the reconstruction of tracks, which led to subtle event-wide correlations that prevented a reliable prediction of the background arising from low-charge jets in QCD multijet events.

With these inefficiencies later recovered in the second half of 2016, a dataset corresponding to 16.1 fb^{-1} was recorded that was used for this analysis, where events are required to pass an online selection algorithm (trigger) asking one jet to have $p_{\text{T}} > 450\,\text{GeV}$. More details on the CMS trigger system can be found in Ref. [23].

The events are required to have two back-to-back jets with low ChF. As a baseline selection, we require two jets with $p_{\text{T}} > 550\,\text{GeV}$, such that the applied trigger requirements are almost fully efficient for the selected events. Furthermore, we require these jets to have $|\eta| < 2.0$, so they are fully within the tracking volume, thus suppressing backgrounds from jets that have a low ChF due to tracks falling out of the tracker acceptance.

Except for the suppressed possibility of SIMPs radiating a mediator splitting back in quarks, SIMPs do not undergo parton showering themselves, while quarks and gluons undergo QCD final state radiation. Therefore, events with SIMPs have a lower number of jets compared to the QCD multijet background. This is illustrated in Figure 2 (top right) which includes jets with $p_{\text{T}} > 30\,\text{GeV}$ and within the acceptance of the calorimeters $|\eta| < 5$. Therefore, we require exactly two such jets in the event, and we select their azimuthal separation to be $\Delta\phi > 2$.

We also apply a photon veto to suppress γ+jets events. This is done by rejecting events where the identified photon with the highest p_{T} falls within $\Delta R = \sqrt{\Delta\eta^2 + \Delta\phi^2} < 0.1$ of the leading or subleading jet. In cases where the jet energy fraction coming from photons is larger than 0.8, but the photon in the jet does not pass the identification requirements, we still reject the event in case a conversion can be found as described in Section 3 within $\Delta R < 0.2$ of the photon. Furthermore, the photon veto is complemented by requiring the two jets to have a neutral electromagnetic energy fraction lower than 0.9.

Finally, we apply an event cleaning selection that mainly removes beam halo events. However, since the jets we aim to select are in a particular phase space usually rejected by jet identification requirements which cannot be used here, other unknown instrumental issues may be enhanced. Therefore, we verified in detail individual events at the smallest ChF values not to be anomalous, both in the QCD multijet simulation as well as in events in the triggered data sample that do not pass the jet p_{T} thresholds,

Figure 2 shows the distributions of the number of jets and the ChF of the two leading jets, for the QCD multijet simulation, and the SIMP signal, obtained after applying these event selection requirements. The different shape of the ChF distribution for QCD simulation and signal stands out.

Starting from this baseline selection, we select a control sample used for the background prediction where at least one of the leading jets has a ChF above 0.25. For this control sample selection, we only apply the ChF requirement on the jets reconstructed using the default primary vertex. The presence of at least one jet with a large ChF avoids the previously described possible wrong choice of the primary vertex.

In the case of the signal selection, the same baseline requirements are applied. Moreover, both the leading and subleading jets are required to have ChF below a certain threshold, assuming both the default and the alternate choice of the primary vertex.

6 Background estimation

The γ+jets background is verified to be negligible and well within any other systematic uncertainty on the background prediction. The photon veto is found to work well, as no events from

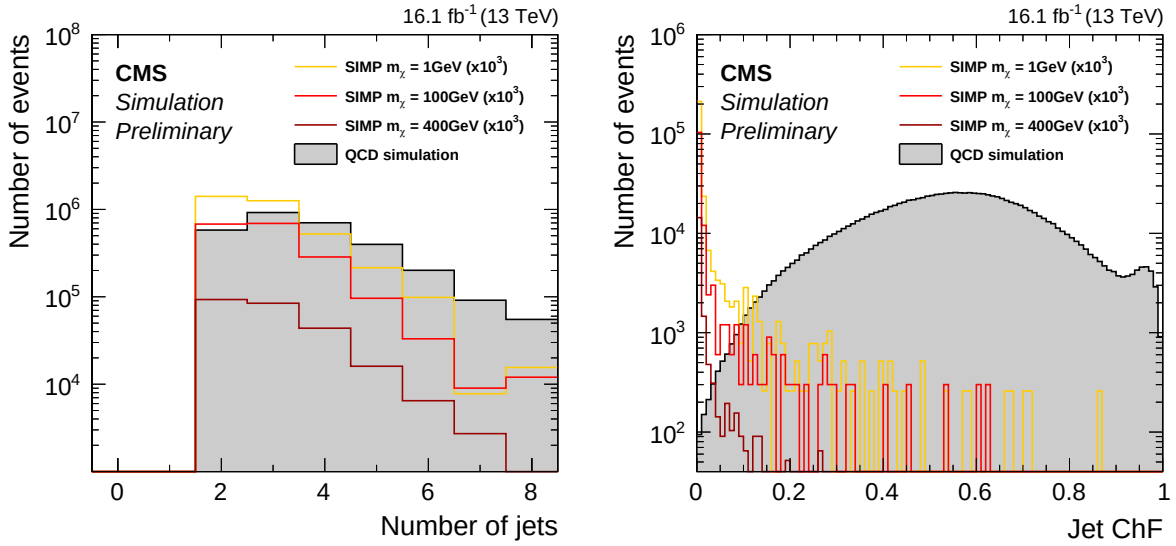

Figure 2: Number of jets with $p_T > 30\,\text{GeV}$ (left) and ChF of the two leading jets (right). The baseline selection is applied, except for the requirement on the number of jets in the corresponding plot. The QCD and SIMP simulations are normalized to 16.1 fb^{-1}.

the simulated sample remain after requiring ChF < 0.1.

For the QCD multijet background, the simulation does not describe the data accurately, especially at low ChF. The differences between the data and the simulation are not problematic, since we estimate the QCD multijet background from data, using simulation to assess the precision of the employed method.

As a first step, we measure the probability of low ChF jets in the control sample, by requiring one jet to have large ChF (ChF > 0.25) and applying the ChF selection on the other jet. This measurement is done in 6 bins of jet p_T and 8 bins of jet η. The number of QCD events in the signal region is then estimated using the QCD dijet events passing the selection requirements described in Section 5, and applying the appropriate p_T and η dependent ChF selection efficiencies on the two leading jets (2-leg prediction). Alternatively, events with one jet with ChF below the signal requirement can be used, where the measured efficiencies are then applied on the other jet (1-leg prediction).

As a first check, a closure test is performed on the background prediction method using jets clustered from particles at the generator level, before interaction with the detector. Excellent agreement is found between the MC truth and the 1-leg and 2-leg predictions, where the MC truth is the yield from simulation after applying the ChF requirement on both jets of generated particles. This confirms that no relevant physical correlations are present between the two jets, and confirms that the choice of p_T and η binning of the ChF efficiencies is adequate.

A further closure test is done by comparing the MC truth with the 1-leg and 2-leg predictions using reconstructed objects in the simulation, as shown in Figure 3. For the MC truth, the ChF selection is applied on the two leading jets of the standard jet collection, as well as the two leading jets of the jet collection created when using the second vertex as primary vertex. As explained, this removes events where the wrong primary vertex choice leads to jets incorrectly reconstructed as being neutral. As can be seen, the method predicts the multijet background within the statistical precision of the test, which shows no significant correlations between the jets are introduced by the event reconstruction. The systematic uncertainty on the background

prediction is then taken as the larger of the statistical uncertainty of the test and the difference between the MC truth and the prediction.

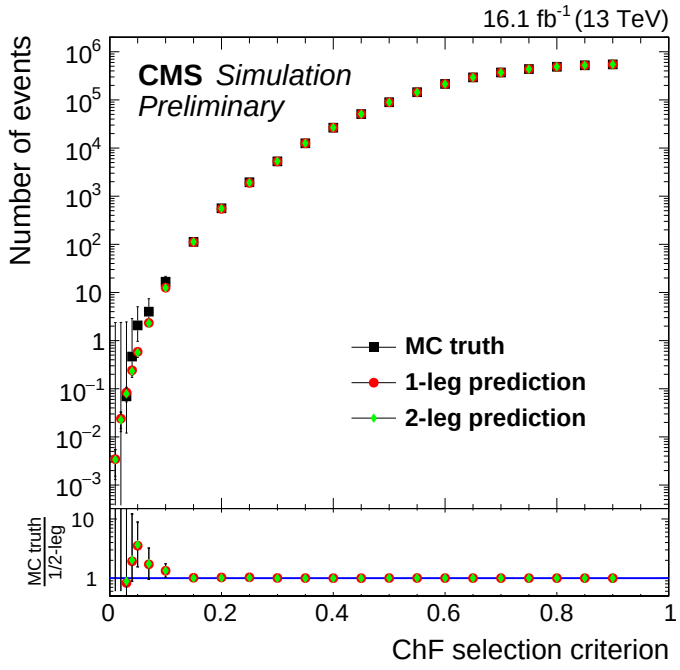

Figure 3: Closure test in MC, as a function of inclusive ChF $< x$ bins.

Next, we perform the prediction using data and compare to the data observation. To demonstrate closure of the method in data without a distraction from a potential signal at low ChF, this comparison is done using exclusive bins in ChF, where the ChF of both leading jets must be below the the upper ChF bin threshold, and one of these above the lower threshold of the bin. This comparison is shown in Figure 4. The 1-leg and 2-leg predictions agree very well in data, confirming also here no correlations between the jets are present. The agreement demonstrates an excellent prediction of the bulk of the ChF distribution and the normalization of the background.

Apart from the physical sources of photon and QCD multijet background, other sources of more instrumental or algorithmic nature may arise, e.g. the mentioned subtlety related to the selection of the correct primary vertex. To ensure the background prediction method does not underestimate such additional spurious sources of background, detailed checks were performed on the events with lowest ChF jets in simulation, as well as in a slightly larger data sample collected with the same trigger, but not passing the offline jet p_{T} requirements. During these checks, no anomalous events were observed passing the earlier described event selection.

7 Results

Table 1 shows the number of predicted and observed events as well as the expected yield from the SIMP signal for two different SIMP masses, for various values of the ChF requirement. The systematic uncertainty on the data prediction is dominated by the closure test. Additionally, the 2% inefficiency of the trigger at the jet p_{T} requirement of 550 GeV is also taken into account in this uncertainty. The result is obtained using the 2-leg prediction, since it has a nearly identical statistical uncertainty as the 1-leg prediction, but avoids the non-trivial statistical overlap

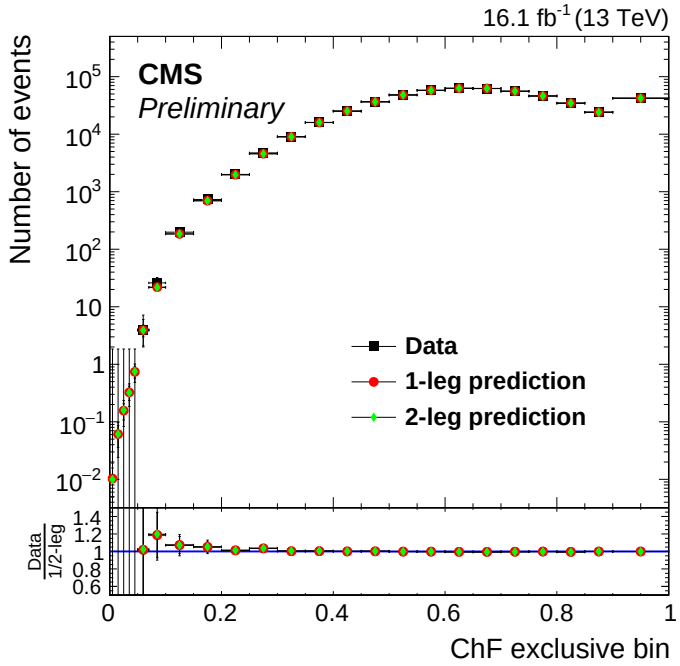

Figure 4: The 1- and 2-leg predictions from data, as well as the direct observation in data, as a function of exclusive bins in ChF, where either the leading or the subleading jet has a ChF within the bin range, and both have a ChF below the upper threshold.

between the event sample used for the binned efficiency measurements, and the one to which the same efficiencies are applied to obtain the prediction.

The signal region from which we derive the interpretations is defined by ChF < 0.05. This rejects most of the QCD background, while avoiding tighter ChF requirements where the MC truth used in the closure tests starts to yield large statistical uncertainties, and where higher-order contributions from mediator radiation off the SIMPs could become non-negligible.

Table 1: Number of predicted (using the 1-leg prediction from data) and observed events for the considered selections. The expected number of signal events is also given for the $m_\chi = 1$ GeV and $m_\chi = 1000$ GeV scenarios, with the corresponding statistical uncertainties.

ChF selection criterion	data prediction	observed	SIMP signal [m_χ]	
			1 GeV	1000 GeV
< 0.2	898 ± 30 (stat.) ± 33 (syst.)	969	1300 ± 58	2.25 ± 0.07
< 0.15	209 ± 10 (stat.) ± 17 (syst.)	229	1269 ± 57	2.18 ± 0.07
< 0.1	26.6 ± 2.2 (stat.) ± 9.3 (syst.)	30	1197 ± 56	2.09 ± 0.07
< 0.07	5.1 ± 0.6 (stat.) ± 4.1 (syst.)	4	1153 ± 55	2.00 ± 0.07
< 0.05	1.28 ± 0.22 (stat.) $^{+3.40}_{-1.28}$ (syst.)	0	1101 ± 53	1.90 ± 0.06

Using these results, we calculate model-independent limits at 95% confidence level (CL) for a ChF < 0.05 selection requirement, using the CL_S criterion with the LHC style test statistic in which the systematic uncertainties are modeled as nuisance parameters [24, 25]. All included systematic uncertainties are profiled with a lognormal prior, except for the uncertainty coming from the closure test, which is profiled with a gamma function since it comes from a limited number of events. This results in an observed (expected) fiducial cross section upper limit of

$\sigma_{\text{fid}}^{95\%} = \sigma \times \text{A} \times \epsilon = 0.18\ (0.18)$ fb.

For the SIMP signals, as is done for data events, the event selection requirements are applied on the new jet collection, which was obtained with respect to the second vertex, as well as on the standard collection, to remove events with a wrong primary vertex choice. The 95% CL cross section upper limits on the SIMP production cross section for $|\eta(\chi)| < 2.5$ and $p_{\text{T}}(\chi) > 200$ GeV are then calculated for SIMP masses between 1 and 1000 GeV, for the signal region with ChF < 0.05, using the same procedure as described for the model-independent limit. The systematic uncertainties included for the signal are the jet energy corrections, the integrated luminosity [26], and the trigger inefficiency. These systematic uncertainties are summarized in Table 2. The photon and conversion veto was found to be 100% efficient on the signal, and this systematic is therefore found to be negligible. The effect of pileup was considered to be negligible, as the distribution of the number of vertices is very similar for the data and SIMP samples. As an example, the data was compared to the SIMP sample with $m_\chi = 1000$ GeV, which showed there is a good agreement in the bulk of the distribution with some deviations in the tails only. The results are shown in Figure 5, and the search is found to exclude SIMP masses up to 900 GeV.

Table 2: The systematic uncertainties taken into account for the signal simulation.

source	uncertainty
jet energy corrections	2.2 - 5.4%
integrated luminosity	2.5%
trigger inefficiency	2%

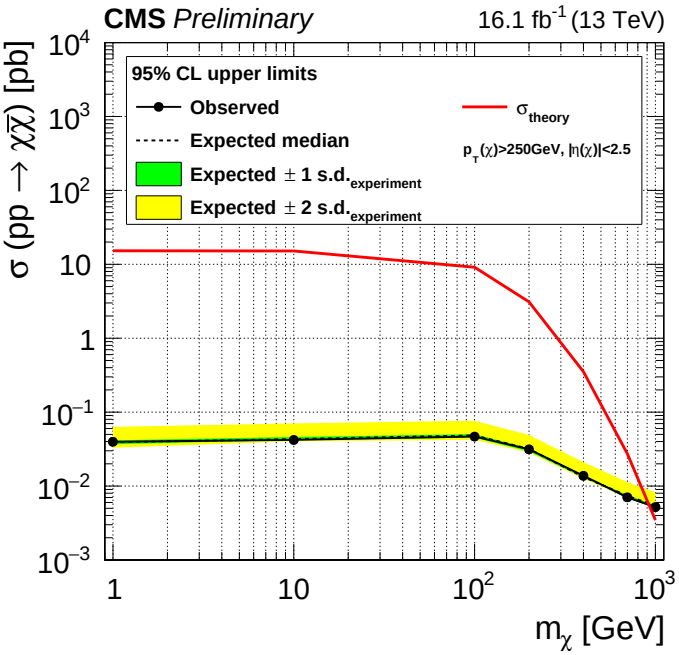

Figure 5: The expected 95% CL upper limits on the production cross section for SIMPs with masses between 1 and 1000 GeV, as well as the theoretical prediction (red), with respect to the generator level selection ($p_T^\chi > 200$ GeV and $|\eta_\chi| < 2.5$).

8 Summary

A search was presented for dark matter in the form of strongly interacting massive particles (SIMPs) manifesting themselves in the detector as a pair of jets without tracks. The large multijet background is efficiently suppressed using the charged energy fraction of jets as the key discriminator. The remaining background is estimated directly from data. Using proton–proton collision data corresponding to an integrated luminosity of 16.1 fb^{-1} of integrated luminosity collected by the CMS experiment in 2016, we set first limits on a potential SIMP signal, excluding SIMP masses up to 900 GeV at 95% confidence level. A model-independent fiducial cross section upper limit of 0.18 fb at 95% confidence level is also provided for a generic fiducial signal of high-momentum trackless jets. The presented analysis thus evaluates the sensitivity to an unconventional phase space for new physics for the first time at colliders, providing both the interpretation in the context of the SIMP model, as well as model-independent limits that can be used for reinterpretation of the results.

References

[1] E. W. Kolb and M. S. Turner, "The Early Universe", *Front. Phys.* **69** (1990) 1.

[2] G. Bertone and D. Hooper, "History of dark matter", *Rev. Mod. Phys.* **90** (2018), no. 4, 045002, doi:10.1103/RevModPhys.90.045002, arXiv:1605.04909.

[3] N. Daci et al., "Simplified SIMPs and the LHC", *JHEP* **11** (2015) 108, doi:10.1007/JHEP11(2015)108, arXiv:1503.05505.

[4] ATLAS Collaboration, "Search for long-lived neutral particles in p p collisions at $\sqrt{s}$ = 13 TeV that decay into displaced hadronic jets in the ATLAS calorimeter", *Eur. Phys. J. C* **79** (2019), no. 6, 481, doi:10.1140/epjc/s10052-019-6962-6, arXiv:1902.03094.

[5] J. H. Davis, "Probing Sub-GeV Mass Strongly Interacting Dark Matter with a Low-Threshold Surface Experiment", *Phys. Rev. Lett.* **119** (2017), no. 21, 211302, doi:10.1103/PhysRevLett.119.211302, arXiv:1708.01484.

[6] CRESST Collaboration, "Results on MeV-scale dark matter from a gram-scale cryogenic calorimeter operated above ground", *Eur. Phys. J. C* **77** (2017), no. 9, 637, doi:10.1140/epjc/s10052-017-5223-9, arXiv:1707.06749.

[7] EDELWEISS Collaboration, "Searching for low-mass dark matter particles with a massive Ge bolometer operated above-ground", *Phys. Rev. D* **99** (2019), no. 8, 082003, doi:10.1103/PhysRevD.99.082003, arXiv:1901.03588.

[8] D. Hooper and S. D. McDermott, "Robust Constraints and Novel Gamma-Ray Signatures of Dark Matter That Interacts Strongly With Nucleons", *Phys. Rev. D* **97** (2018), no. 11, 115006, doi:10.1103/PhysRevD.97.115006, arXiv:1802.03025.

[9] T. Emken and C. Kouvaris, "How blind are underground and surface detectors to strongly interacting Dark Matter?", *Phys. Rev. D* **97** (2018), no. 11, 115047, doi:10.1103/PhysRevD.97.115047, arXiv:1802.04764.

[10] CMS Collaboration, "The CMS experiment at the CERN LHC", *JINST* **3** (2008) S08004, doi:10.1088/1748-0221/3/08/S08004.

[11] CMS Collaboration, "Particle-flow reconstruction and global event description with the CMS detector", *JINST* **12** (2017), no. 10, P10003, doi:10.1088/1748-0221/12/10/P10003, arXiv:1706.04965.

[12] M. Cacciari, G. P. Salam, and G. Soyez, "The Anti-k(t) jet clustering algorithm", *JHEP* **04** (2008) 063, doi:10.1088/1126-6708/2008/04/063, arXiv:0802.1189.

[13] M. Cacciari, G. P. Salam, and G. Soyez, "FastJet user manual", *Eur. Phys. J. C* **72** (2012) 1896, doi:10.1140/epjc/s10052-012-1896-2, arXiv:1111.6097.

[14] CMS Collaboration, "Jet energy scale and resolution in the CMS experiment in pp collisions at 8 TeV", *JINST* **12** (2017), no. 02, P02014, doi:10.1088/1748-0221/12/02/P02014, arXiv:1607.03663.

[15] CMS Collaboration, "Description and performance of track and primary-vertex reconstruction with the CMS tracker", *JINST* **9** (2014), no. 10, P10009, doi:10.1088/1748-0221/9/10/P10009, arXiv:1405.6569.

[16] CMS Collaboration, "Technical proposal for the phase-ii upgrade of the compact muon solenoid", CMS Technical proposal CERN-LHCC-2015-010, CMS-TDR-15-02, CERN, 2015.

[17] CMS Collaboration, "Performance of Photon Reconstruction and Identification with the CMS Detector in Proton-Proton Collisions at $\sqrt{s} = 8$ TeV", *JINST* **10** (2015), no. 08, P08010, doi:10.1088/1748-0221/10/08/P08010, arXiv:1502.02702.

[18] A. Alloul et al., "FeynRules 2.0 - A complete toolbox for tree-level phenomenology", *Comput. Phys. Commun.* **185** (2014) 2250, doi:10.1016/j.cpc.2014.04.012, arXiv:1310.1921.

[19] J. Alwall et al., "The automated computation of tree-level and next-to-leading order differential cross sections, and their matching to parton shower simulations", *JHEP* **07** (2014) 079, doi:10.1007/JHEP07(2014)079, arXiv:1405.0301.

[20] T. Sjöstrand et al., "An Introduction to PYTHIA 8.2", *Comput. Phys. Commun.* **191** (2015) 159, doi:10.1016/j.cpc.2015.01.024, arXiv:1410.3012.

[21] CMS Collaboration, "Event generator tunes obtained from underlying event and multiparton scattering measurements", *Eur. Phys. J. C* **76** (2016), no. 3, 155, doi:10.1140/epjc/s10052-016-3988-x, arXiv:1512.00815.

[22] GEANT4 Collaboration, "GEANT4: A Simulation toolkit", *Nucl. Instrum. Meth. A* **506** (2003) 250, doi:10.1016/S0168-9002(03)01368-8.

[23] CMS Collaboration, "The CMS trigger system", *JINST* **12** (2017), no. 01, P01020, doi:10.1088/1748-0221/12/01/P01020, arXiv:1609.02366.

[24] A. L. Read, "Presentation of search results: the cls technique", *J. Phys. G* **28** (2002) 2693, doi:10.1088/0954-3899/28/10/313.

[25] T. Junk, "Confidence level computation for combining searches with small statistics", *Nucl. Instrum. Meth. A* **434** (1999) 435, doi:10.1016/S0168-9002(99)00498-2, arXiv:hep-ex/9902006.

[26] CMS Collaboration, "CMS Luminosity Measurements for the 2016 Data Taking Period", CMS Physics Analysis Summary CMS-PAS-LUM-17-001, 2017.